ORIGINAL ARTICLE

European Journal of **Soil Science** **WILEY**

Relations between soil organic carbon content and the pore size distribution for an arable topsoil with large variations in soil properties

Jumpei Fukumasu[1] | Nick Jarvis[1] | John Koestel[1,2] | Thomas Kätterer[3] | Mats Larsbo[1]

[1]Department of Soil and Environment, Swedish University of Agricultural Sciences (SLU), Uppsala, Sweden

[2]Soil Quality and Soil Use, Agroscope, Zürich, Switzerland

[3]Department of Ecology, Swedish University of Agricultural Sciences (SLU), Uppsala, Sweden

Correspondence
Jumpei Fukumasu, Department of Soil and Environment, Swedish University of Agricultural Sciences (SLU), Box 7014, 750 07 Uppsala, Sweden.
Email: jumpei.fukumasu@slu.se

Abstract

Soil organic carbon (SOC) in arable topsoil is known to have beneficial effects on soil physical properties that are important for soil fertility. The effects of SOC content on soil aggregate stability have been well documented; however, few studies have investigated its relationship with the soil pore structure, which has a strong influence on water dynamics and biogeochemical cycling. In the present study, we examined the relationships between SOC and clay contents and pore size distributions (PSDs) across an arable field with large spatial variations in topsoil SOC and clay contents by combining X-ray tomography and measurements of soil water retention. Additionally, we investigated the relationships between fractionated SOC, reactive Fe and Al oxide contents and soil pore structure. We found that porosities in the 0.2–720 μm diameter class were positively correlated with SOC content. A unit increase of SOC content was associated with a relatively large increase in porosity in the 0.2–5 and 480–720 μm diameter classes, which indicates that enhanced SOC content would increase plant available water content and unsaturated hydraulic conductivity. On the other hand, macroporosities (1200–3120 μm diameter classes) and bioporosity were positively correlated with clay content but not with SOC content. Due to strong correlations between soil texture, carbon-to-nitrogen ratios and reactive iron contents, we could not separate the relative importance of these soil properties for PSDs. Reactive aluminium and particulate organic carbon contents were poorer predictors for PSDs compared with clay and SOC contents. This study provides new insights on the relations between SOC and soil pore structure in an arable soil and may lead to improved estimations of the effects of enhanced SOC sequestration on soil water dynamics and soil water supply to crops.

Highlights

• Relations between soil organic carbon (SOC) and pore size distribution (PSD) in an arable soil were explored.

- We used X-ray tomography and soil water retention to quantify a wide range of PSD.
- There were positive correlations between SOC and porosities in 0.2–720 μm diameter classes.
- Porosities in 0.2–5 and 480–720 μm diameter classes were more strongly correlated with SOC than clay.
- Our results have implications for improved estimates of effects of SOC sequestration on soil water dynamics.

1 | INTRODUCTION

Although the soil organic carbon (SOC) content in arable soils changes slowly (e.g., Franko & Schulz, 2021), the promotion of policies for carbon (C) sequestration in agricultural soils has received attention as a strategy to mitigate climate change and global warming (Chenu et al., 2019) and restore the physical quality of degraded arable soils (Fell et al., 2018; Jensen et al., 2019; Johannes et al., 2017). The effects of SOC and different organic amendments on aggregate stability have been extensively studied (e.g., Abiven et al., 2009; Bronick & Lal, 2005; Chenu et al., 2000; King et al., 2019). For example, Chenu et al. (2000) reported a positive correlation between SOC and mean weight diameter of water-stable aggregates mainly due to decreased water wettability of aggregates with larger SOC content. However, much less is known about the effects of SOC on the soil pore structure, which is an important component of soil physical quality, since it influences many critical soil properties and processes including the transport and retention of water and solutes and biogeochemical cycling (Rabot et al., 2018). In turn, the soil pore structure itself influences the long-term stabilisation of SOC, because it regulates microbial accessibility to SOC and hence its rate of decomposition (Dungait et al., 2012; Kravchenko & Guber, 2017; Ruamps et al., 2011; Strong et al., 2004). For example, using X-ray tomography, Kravchenko et al. (2015) reported that a greater abundance of connected pores >13 μm in diameter led to a faster rate of decomposition of intra-aggregate particulate organic matter (POM). Recently, Meurer, Chenu, et al. (2020) developed a model of these two-way interactions between SOC content and soil pore structure, which was successfully tested against a dataset from a long-term field experiment.

Several studies have shown negative correlations between SOC and bulk density (e.g., Kätterer et al., 2006; Meurer, Chenu, et al., 2020; Ruehlmann &

Körschens, 2009), which suggests that larger SOC results in larger total porosity (assuming constant particle density). Effects of SOC on pore size distributions (PSDs), which can be estimated from soil water retention, are not as clear. At national and continental scales, volumetric water contents at field capacity and wilting point and parameters of water retention functions have been shown to be strongly correlated with soil texture (i.e., clay content) but only weakly or not at all correlated with SOC content (Kätterer et al., 2006; Nemes et al., 2005; Rawls et al., 2003; Zacharias & Wessolek, 2007). Additionally, while positive correlations between SOC and plant available water content (PAWC, i.e., the difference between water contents at field capacity and wilting point) were reported by some authors (e.g., Hudson, 1994; Olness & Archer, 2005), recent global- and continental-scale data analyses reported only limited effects of SOC on PAWC (Libohova et al., 2018; Minasny & McBratney, 2018a). Lal (2020) recently summarised previous research on the effects of SOC on PAWC and suggested that more research was needed to explain these apparently contradictory findings. He suggested that the extent of increases in PAWC with increased SOC content may depend on soil texture and the initial SOC content. Minasny and McBratney (Minasny & McBratney, 2018a, 2018b) suggested that the effects of SOC can be larger on air-filled porosity at field capacity (i.e., porosity >10 μm diameter) than on PAWC. These studies also indicated the need to assess associations between SOC and wide ranges of PSDs. To the best of our knowledge, there are only a few studies that report relationships between SOC and porosities in pore size classes using soil water retention (Minasny & McBratney, 2018b). For example, in a long-term experiment, Kirchmann and Gerzabek (1999) reported a strong positive correlation between SOC and the porosity in the 1–3 μm diameter class, whereas porosities in the >60 μm diameter class were not correlated with SOC content. It should be noted that in their study,

the variation in SOC contents were caused by different soil management practices (i.e., organic and inorganic fertilisation and cropping vs. bare fallow), which can be confounding factors when studying associations between SOC and PSD.

With the advent of X-ray tomography, the relationships between SOC and macropore size distribution have been reported in several studies (e.g., Jarvis et al., 2017; Naveed et al., 2014; Paradelo et al., 2016; Xu et al., 2018). For example, Jarvis et al. (2017) observed no significant correlation between SOC content and X-ray visible porosity (pore diameters >65 μm), while total porosities were strongly and positively correlated with SOC content. These results led them to the conclusion that enhanced SOC content through long-term inclusions of grass-clover leys in the crop rotation resulted in an increase of soil matrix pores with diameters smaller than 65 μm. In a soil under grass ley, Larsbo et al. (2016) found a significant positive correlation between SOC content and X-ray imaged porosity for pores in the smallest imaged size class (200–600 μm in diameter), but none for pores larger than 600 μm in diameter. Larger soil macropores are created by soil biological activity (e.g., root growth and decay and faunal burrowing, e.g., Lucas et al., 2019; Meurer, Barron, et al., 2020) and, in arable soils, by tillage operations. Both soil fauna and roots are of major importance for SOC turnover in soil. In turn, biological activity is affected by soil texture and SOC (e.g., Holmstrup et al., 2011; Klok et al., 2007; Le Couteulx et al., 2015; Poeplau & Kätterer, 2017). Quantification of soil biopores may, hence, provide additional information on the interactions between SOC and soil structure. Recently, methods have been developed to separate biopores from the total macroporosity in X-ray tomography images (Lucas et al., 2019).

Reactive oxides are known to be important as cementing and binding agents of clay and SOC due to their large specific surface area and variable charges (Six et al., 2004; Totsche et al., 2018). Many studies have demonstrated the stabilising effects of reactive oxides on the formation of the so-called micro-aggregates (e.g., Asano & Wagai, 2014; Grønsten & Børresen, 2009), but few studies have investigated their effects on soil porosity in arable soils. One exception is Regelink et al. (2015), who reported a positive correlation between oxalate-extractable iron (Feox) and porosities <1000 μm diameter class for soils taken from three European sites. They proposed a conceptual model whereby an Fe-bearing reactive mineral phase was a key component in the aggregation of clay and silt-sized particles and in the formation of <9 μm sized porosity. In addition, Shoji et al. (1996) reported a strong positive correlation between water content at wilting point and reactive aluminium (Al) and Fe contents for Japanese Andisols. These studies suggest that the reactive oxide content of soil may also be an important determinant of soil pore structure.

Organic matter in soils is often fractionated into POM and organic matter associated with the silt- and clay-sized (SC) fractions; the POM fraction consists of relatively young, fresh soil organic matter (SOM) and hence may be a good diagnostic indicator for short-term changes in SOC, while SOC associated with the SC fraction may be more stable against microbial decomposition and hence important for long-term SOC stabilisation (Lavallee et al., 2020; Poeplau et al., 2018; Rocci et al., 2021). Although relationships between these SOC fractions and aggregate stability have been well investigated (Jastrow et al., 2007; Jensen et al., 2019; Six et al., 2004), their relationships with soil pore structure have, to the best of our knowledge, not yet been explored.

The objective of the present study was to reveal relationships between SOC and PSD. To do so, we sampled the topsoil from an arable field with a large variation in SOC and clay contents (Fukumasu et al., 2021; Lindahl et al., 2008). The management across the field, which could potentially influence soil pore structure, has been similar during the last 60 years. We combined X-ray tomography imaging and measurements of soil water retention to quantify PSDs across a wide range. In addition to SOC content and soil texture, we measured proxies of Al- and Fe-bearing reactive mineral phases and SOC in soil fractions to examine their relations with PSDs. We chose to investigate this question at the field scale instead of the regional scale or using plot experiments with different treatments in order to eliminate differences in land management (e.g., crop types and rotations, tillage systems, organic fertilizations) and climate, which could potentially mask the relationships between SOC and soil pore structure. The large within-field variations in soil texture and SOC allowed us to investigate their roles for pore structure formation.

2 | MATERIALS AND METHODS

2.1 | Site description and soil sampling

The studied field (46.9 ha) is located on the Bjertorp farm in Västergötland (58°14′00.0″N 13°08′00.0″E), south-west Sweden (Lindahl et al., 2008). Details of the site are presented in Fukumasu et al. (2021). Briefly, this field has been cultivated for at least 60 years with barley, oats, rape and wheat as major crops. Soil management has been similar across the field except that different crops were grown in parts of the field for some years, and precision fertilisation of nitrogen, phosphorus and potassium was practiced in some years. Based on the World Reference

Base (2015) system, soil profiles at three locations in the field were classified as Stagnic Eutric Cambisol, Eutric Stagnosol and Haplic Phaeozem. Mean annual precipitation and temperature are 624 mm and 7.3°C, respectively (average for the period 2006–2019 taken from the nearby metrological station at Hällum, Swedish Meteorological and Hydrological Institute). In late August 2017, after the harvest of rape but before tillage, two different sized intact soil cores and one sample of loose soil were taken as close to each other as possible (within 30 cm) at 35 locations selected using stratified sampling to cover the range of combinations of SOC and clay contents found in a previous soil sampling campaign (Lindahl et al., 2008; Figure S1). Large intact samples were taken in polyvinyl chloride (PVC) cylinders (20 cm height, 12.5 cm diameter) from the uppermost ca. 17 cm of soil using a tractor-mounted hydraulic press. Small intact samples were taken in steel cylinders (10 cm height, 6.8 cm diameter) at a depth of ca. 3–13 cm using a drop hammer. The large samples were first scanned using X-ray tomography. The samples were then used for non-reactive solute transport experiment (data not shown here). After these experiments, soil from within the columns was extracted from depths of ca. 3–13 cm, air-dried at ca. 38°C, crushed and sieved to <2 mm. These samples were then used for soil texture analysis, SOC fractionation and oxalate extraction of Al and Fe. The small cylinder samples were used to determine dry bulk density and soil water retention. The loose soil was air-dried at ca. 38°C, crushed and sieved to <2 mm, and then used for measurements of water content at wilting point. We refer to the sieved soil samples as bulk soil.

2.2 | Basic soil properties and SOM fractionation

Soil texture (sand: 60–2000 μm, silt: 2–60 μm, clay: <2 μm) was determined by wet-sieving and by the pipette method using ca. 20 g of bulk soil. Before texture analysis, SOM was removed by 10 ml peroxide (35%) and the soil was dispersed by adding 25 ml of chemical dispersant (7 g L^{-1} sodium carbonate, Na_2CO_3 + 33 g L^{-1} sodium metaphosphate, $(NaPO_3)_n$). Al- and Fe-bearing reactive mineral phases were estimated after oxalate extraction; 1 g of dried soil was extracted in the dark by 100 ml of oxalate extraction solution (0.2 mol/L oxalate, mixture of 4.8 L ammonium oxalate solution and 3.6 L oxalic acid solution, pH adjusted to 3.0). The reactive Al and Fe contents were then measured using inductivity coupled plasma optical emission spectrometer.

SOM fractionation as developed by Zimmermann et al. (2007) and modified by Poeplau et al. (2013) was

conducted to isolate SOC associated with different particle size classes. The details of the method are given on page S10 in the supplementary materials. The fractionation resulted in four distinctive fractions, namely POM, SOM associated with the sand-sized fraction (>63 μm), SOM associated with the silt + clay (SC) sized fraction (<63 μm) and SOM that is resistant to oxidation (rSOM). SOC and N contents in SOM fractions were measured by dry-combustion on a TruMac CN (LECO Corp.). The inorganic carbon content was negligible (i.e., <0.024 g C kg^{-1} bulk soil; Fukumasu et al., 2021). The carbon-to-nitrogen (C:N) ratios were similar in the sand-sized fraction and in the POM fraction (Fukumasu et al., 2021). We therefore used the SOC content and the C:N ratio in the combined sand and POM fraction. From here on we refer to the C content in this fraction as POM-C. SOC in the SC-sized fraction and rSOM fraction on a bulk soil basis (g kg^{-1} bulk soil) were strongly positively correlated with the total SOC content (Fukumasu et al., 2021). We therefore used only the total SOC content (referred to as SOC from here on) and POM-C in the statistical analyses described below. We used the C:N ratio of bulk SOM and POM as an indicator for the degree of microbial decomposition (Gregorich et al., 2006). It should be noted that the C:N ratio of bulk SOM was strongly positively correlated with that of SOM in the SC fraction (Figure S2). SOC content and POM contents were weakly but negatively correlated with clay content (Figure 1a,c). SOC content in the SC fraction (SC-C) was strongly and positively correlated with SOC content, while POM-C content was positively but only weakly correlated with SOC content (Figure 1b,d). A statistical summary of soil properties is shown in Table S1. A Spearman correlation matrix of the soil properties, which shows that some of the variables are correlated with one another, is presented in Figure 2.

2.3 | X-ray tomography

The X-ray scanning was conducted using the GE Phoenix X-ray scanner (v|tome|x 240) installed at the Department of Soil and Environment at the Swedish University of Agricultural Sciences, Uppsala. The X-ray scanner has a tungsten target, a 240-kV X-ray tube and a GE 16″ flat panel detector. Exactly 2000 radiographs were collected for each of the large intact soil columns at a voltage of 180 kV, a current of 630 μA and exposure time of 333 μs for samples with clay content <30% and 170 kV, 740 μA and 1000 μs for samples with clay content >30% respectively. A three-dimensional image was constructed from the radiographs using the GE image reconstruction software datos|x 2.1.0 RTM. The resulting voxel edge length was 120 μm in all directions, which means that we can

FIGURE 1 Relationships between (a) clay and SOC contents, (b) SC-C and SOC contents, (c) POM-C and clay content and (d) POM-C and SOC content. The yellow line in (b) is the 1:1 line. The unit for SOC, POM-C and SC-C is g C kg^{-1} bulk soil. POM-C, SOC content in the particulate organic matter fraction; SOC, soil organic carbon; SC-C: SOC content in the silt + clay sized fraction
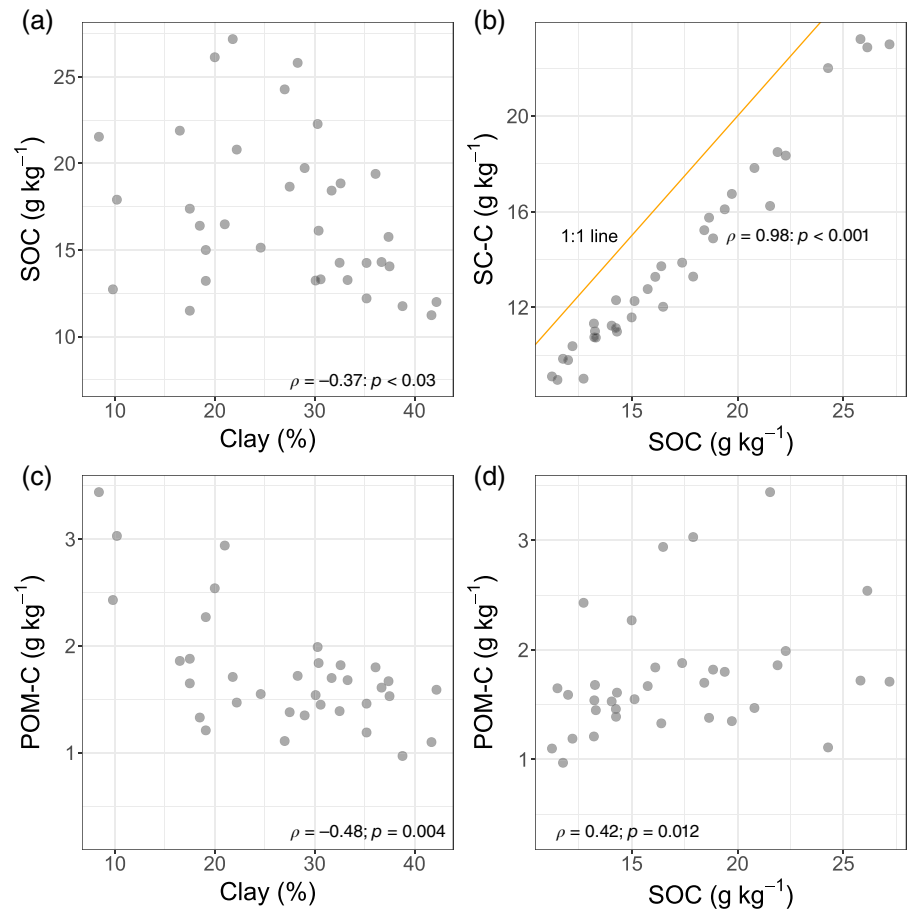
detect pores with diameters larger than approximately 240 μm. We used a cylindrical region of interest 8.4 cm in diameter at the 3.0–13.0 cm depth to exclude artificial pores located close to the PVC wall, which were likely created during soil sampling. Since the soil surfaces were uneven, we defined the location of the surface where the solid phase filled 50% of the horizontal cross-section area (Larsbo et al., 2014).

2.4 | Image processing and analysis

We carried out image processing using the open-source software ImageJ and the bundle of plugins included in FIJI (Schindelin et al., 2012). We applied a three-dimensional median filter with a radius of 1 to the images to reduce noise. We then corrected illumination differences between images and within images in the vertical direction using the plugin SoilJ (Koestel, 2018) with the grey values in the wall of the PVC cylinders and the air inside the columns as references. We used a single grey value threshold to segment all images into pore voxels and solid-phase voxels. Since the automatic thresholding methods included in ImageJ did not result in a satisfactory segmentation of pores and solids, we determined the threshold value by

visually comparing grey value images and binary images. With the chosen threshold, we assigned POM to the pore phase. Total visible porosities and PSDs were then calculated using SoilJ. We also identified biopores using the method proposed by Lucas et al. (2019), which defined all tubular pores as biopores. Briefly, we first reduced the resolution of the binary images by a factor of two to reduce the computation time for the calculations. The eigenvalues of the Hesse matrix (i.e., the tensor of second derivatives of the local grey values) were then calculated after applying Gaussian Blur filters with different standard deviations to the binary images. Eight different standard deviations σ were considered to detect biopores of different diameters. By doing so, tubular pores were separated from irregularly shaped pores. In each calculation, 3D dilations were carried out to better reproduce the actual width of the biopores. Total bioporosity and biopore size distributions were then calculated using SoilJ. We separated macropores and biopores into the following pore diameter classes: 240–480, 480–720, 720–1220, 1220–1920, 1920–3120 and >3120 μm. For biopores, we only analysed pores with diameters larger than 480 μm, due to the above-mentioned resolution reduction. In addition, biopore length density (biopore length per volume of the samples) was calculated assuming that pores segmented as biopores were cylindrical (Lucas et al., 2019).
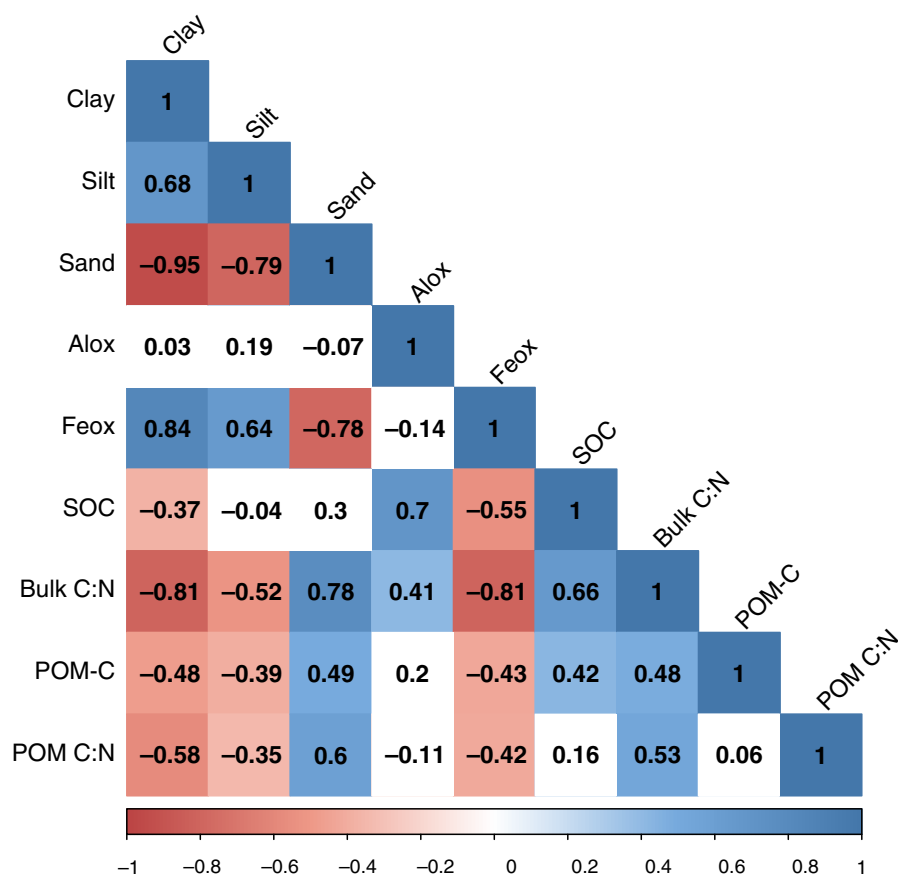
FIGURE 2 Spearman rank correlation matrix of soil properties ($n = 35$). Significant correlations ($p < 0.05$) were highlighted either in red (negative) or in blue (positive). Alox, oxalate-extractable aluminium; bulk C:N, carbon-to-nitrogen ratio of bulk soil organic matter; Feox, oxalate-extractable iron; POM C:N, carbon-to-nitrogen ratio of the particulate organic matter fraction; POM-C, SOC content in the particulate organic matter fraction; SOC, soil organic carbon

2.5 | Soil water retention and pore size distribution

Soil water retention was measured at pressure potentials of −30 and −100 cm on a sand box, at pressure potentials of −300 and −600 cm using a suction plate and at −15,000 cm pressure potential using a pressure plate extractor. For the measurements at wilting point (i.e., −15,000 cm), soils sieved to <2 mm were used. Each pressure potential was then converted to an equivalent pore diameter with the Young–Laplace equation: $d = -3000/\psi$, where d is pore diameter (μm) and ψ is pressure potential (cm). By calculating the difference in volumetric water contents between measurements at different pressure potentials, we estimated the porosity of the following pore diameter classes: >100 μm, 30–100 μm, 10–30 μm, 5–10 μm, 0.2–5 μm and <0.2 μm. Total porosity was then estimated from dry bulk density, assuming a particle density of 2.65 g cm^{-3}.

2.6 | Statistical analysis

We used Spearman rank correlation coefficients to examine the statistical relationships between porosities in different pore diameter classes and soil properties because some

of the soil properties were not normally distributed. We also performed multiple linear regression analysis to determine how the porosities in different diameter classes were influenced by unit changes in SOC and clay contents. Additionally, we determined the relative importance of clay and SOC for explaining the total variance for each pore diameter class using the function "lmg" available in R package "relaimpo" (Grömping & Lehrkamp, 2015). This function decomposes the total variance for each of the multiple linear regression models into contributions made by clay and SOC respectively. Assumptions of normality and homoscedasticity of residuals were visually checked. We used a significance level of $p = 0.05$. All statistical analyses were carried out in R (R Core Team, 2019).

3 | RESULTS

3.1 | Macroporosity and bioporosity quantified by X-ray tomography

The range of total visible porosity quantified by X-ray tomography was 0.062 to 0.224 m^3 m^{-3} (Figure 3a). Porosities were distributed between all pore diameter classes with the largest fraction in the 720–1200 μm diameter class (Figure 3a). Porosities in the 240–480 μm

and 480–720 μm diameters classes were positively correlated with SOC content and with the C:N ratio of bulk SOM, whereas porosities were not correlated with POM-C content and C:N ratios of POM except for positive correlations between the C:N ratio of POM and porosities in the >3120 μm diameter class (Figure 3b). The porosity in the 240–480 μm diameter class was negatively correlated with clay content, whereas porosities in the 1200–3120 μm diameter classes were positively correlated with clay (Figure 3b).

The biopore length density varied between 0.043 and 0.78 cm cm^{-3} (mean 0.40). The total bioporosity varied between 0.0005 and 0.027 m^3 m^{-3}, with larger bioporosities in the two largest diameter classes (Figure 4a). Total bioporosity contributed to about 10% of the total X-ray visible porosity, and the larger the diameter of macropores, the larger the biopore fraction (Figure S3a). Except for the 1200–1920 μm diameter class, total bioporosities and bioporosities in individual diameter classes were not correlated with the corresponding macroporosities (Figure S3b). Total

bioporosity was positively correlated with clay, silt and Feox contents, whereas it was not correlated with SOC content (Figure 4b). The bioporosity in the 480–720 μm diameter class, which constituted a minor fraction of total bioporosity, was positively correlated with SOC (Figure 4b), but this result should be interpreted with care, since such a small porosity may have been affected by some outliers or vulnerable to image noise. Bioporosities in the 720–3120 μm diameter classes were positively correlated with clay, silt and Feox contents while they were negatively correlated with sand, POM-C, and C:N ratios of bulk SOM and POM. These bioporosities were not correlated with SOC. Bioporosities were not correlated with Alox content.

3.2 | Volumetric water content and pore size distribution

Total porosity varied between 0.414 and 0.558 m^3 m^{-3} with relatively large proportions found in the pore
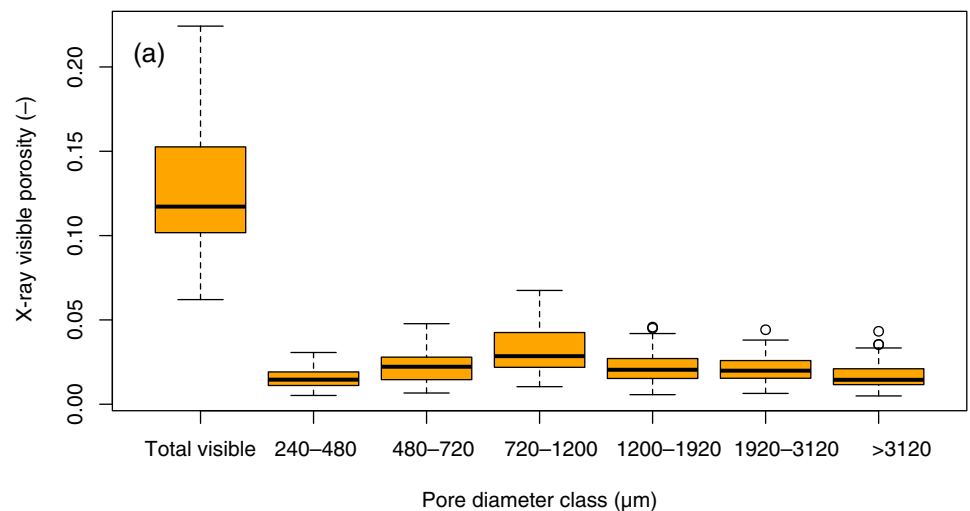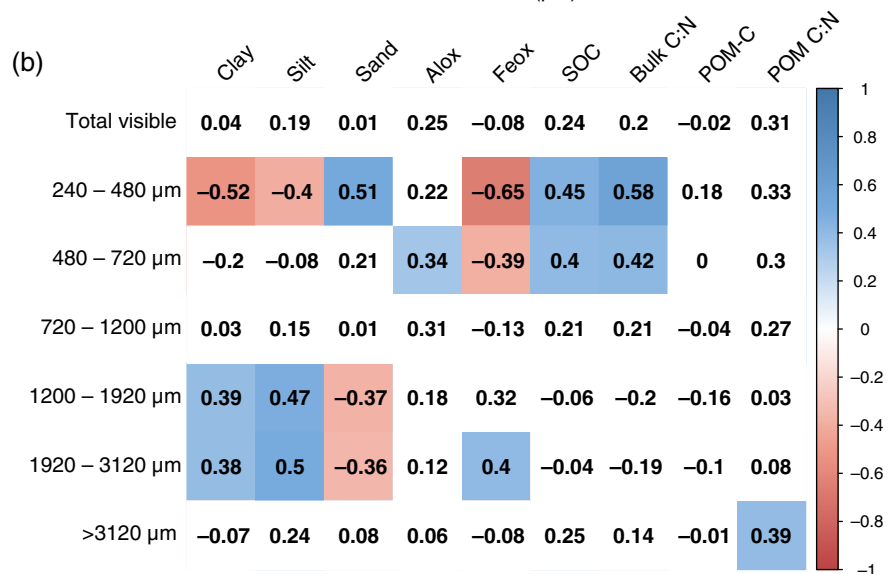

FIGURE 3 Results from X-ray tomography imaging (a) box plot of total visible porosity and porosities in different pore diameter classes and (b) Spearman rank correlation matrix of soil properties and porosities in different pore diameter classes ($n = 35$). Significant correlations ($p < 0.05$) were highlighted either in red (negative) or in blue (positive). Alox, oxalate-extractable aluminium; bulk C:N, carbon-to-nitrogen ratio of bulk soil organic matter; Feox, oxalate-extractable iron; POM C:N, carbon-to-nitrogen ratio of the particulate organic matter fraction; POM-C, SOC content in the particulate organic matter fraction; SOC, soil organic carbon
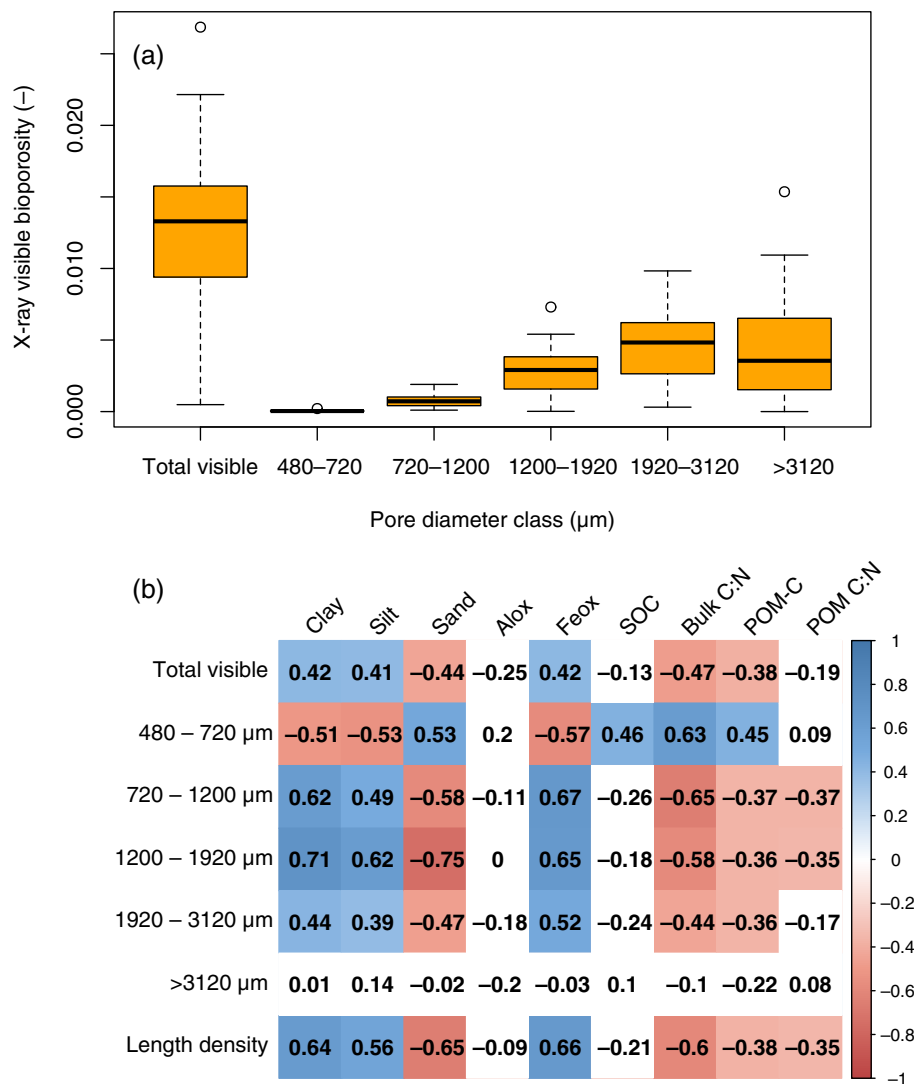
	Clay	Silt	Sand	Alox	Feox	SOC	Bulk C:N	POM-C	POM C:N
Total visible	0.04	0.19	0.01	0.25	−0.08	0.24	0.2	−0.02	0.31
240 – 480 μm	−0.52	−0.4	0.51	0.22	−0.65	0.45	0.58	0.18	0.33
480 – 720 μm	−0.2	−0.08	0.21	0.34	−0.39	0.4	0.42	0	0.3
720 – 1200 μm	0.03	0.15	0.01	0.31	−0.13	0.21	0.21	−0.04	0.27
1200 – 1920 μm	0.39	0.47	−0.37	0.18	0.32	−0.06	−0.2	−0.16	0.03
1920 – 3120 μm	0.38	0.5	−0.36	0.12	0.4	−0.04	−0.19	−0.1	0.08
>3120 μm	−0.07	0.24	0.08	0.06	−0.08	0.25	0.14	−0.01	0.39

FIGURE 4 Results from X-ray tomography imaging (a) box plot of visible bioporosity and bioporosities in different pore diameter classes ($n = 35$) and (b) Spearman rank correlation matrix of soil properties, biopore length density and bioporosities in different pore diameter classes ($n = 35$). Significant correlations ($p < 0.05$) were highlighted either in red (negative) or in blue (positive). Alox, oxalate-extractable aluminium; bulk C:N, carbon-to-nitrogen ratio of bulk soil organic matter; Feox, oxalate-extractable iron; POM C:N, carbon-to-nitrogen ratio of the particulate organic matter fraction; POM-C, SOC content in the particulate organic matter fraction; SOC, soil organic carbon

diameter classes >100 μm, 0.2–5 μm and <0.2 μm compared with the 30–100 μm, 10–30 μm and 5–10 μm diameter classes (Figure 5a). Total porosity and porosities in all pore diameter classes except for the pores <0.2 μm in diameter were positively correlated with SOC content (Figure 5b). Porosities in the pore diameter class of 5–100 μm were also positively correlated with POM-C content (Figure 5b). Porosities in the diameter classes <0.2, 5–10, 10–30 and 30–100 μm were more strongly correlated with clay, sand and Feox contents than SOC content.

The variability in volumetric water contents increased with decreasing pressure potential (Figure S4a). Bulk density and volumetric water content at −30 cm pressure potential were correlated with SOC and Alox contents (Figure S4b). On the other hand, volumetric water contents in the pressure potential range of −100 to −15,000 cm were strongly and positively correlated with clay and Feox contents, while they were negatively correlated with sand, POM-C and C:N ratios of bulk SOM and POM (Figure S4b).

3.3 | Multiple linear regression

The regression coefficients of SOC for porosities in the <0.2, 10–30 and 30–100 μm pore diameter classes were not significant ($p > 0.05$), although the assumption of homoscedasticity of residuals for the models for porosities in the 10–30 and 30–100 μm diameter classes was not met. The porosities in the 10–30 and 30–100 μm diameter classes increased exponentially with clay content (Adj. $R^2 = 0.83$, Figure S5a and Adj. $R^2 = 0.74$, Figure S6a). However, for comparison, we included the results of the multiple linear regressions also for these pore diameter classes in Figure 6.

The regression coefficient for SOC and individual pore diameter classes was largest for the porosity in the 0.2–5 μm pore diameter class, followed by the 480–720, 240–480 and 5–10 μm diameter classes (Figure 6a). There was a large increase in porosity in the <0.2 μm diameter class with a unit increase of clay content, while the porosities in the other diameter classes showed the opposite

FIGURE 5 Results from soil water retention (a) box plot of total porosity and porosities in different pore diameter classes (*n* = 35) and (b) Spearman rank correlation matrix of soil properties and total porosity and porosities in different pore diameter classes (*n* = 35). Significant correlations (*p* < 0.05) were highlighted either in red (negative) or in blue (positive). Alox, oxalate-extractable aluminium; bulk C:N, carbon-to-nitrogen ratio of bulk soil organic matter; Feox, oxalate-extractable iron; POM C:N, carbon-to-nitrogen ratio of the particulate organic matter fraction; POM-C, SOC content in the particulate organic matter fraction; SOC, soil organic carbon; SWR, Soil water retention
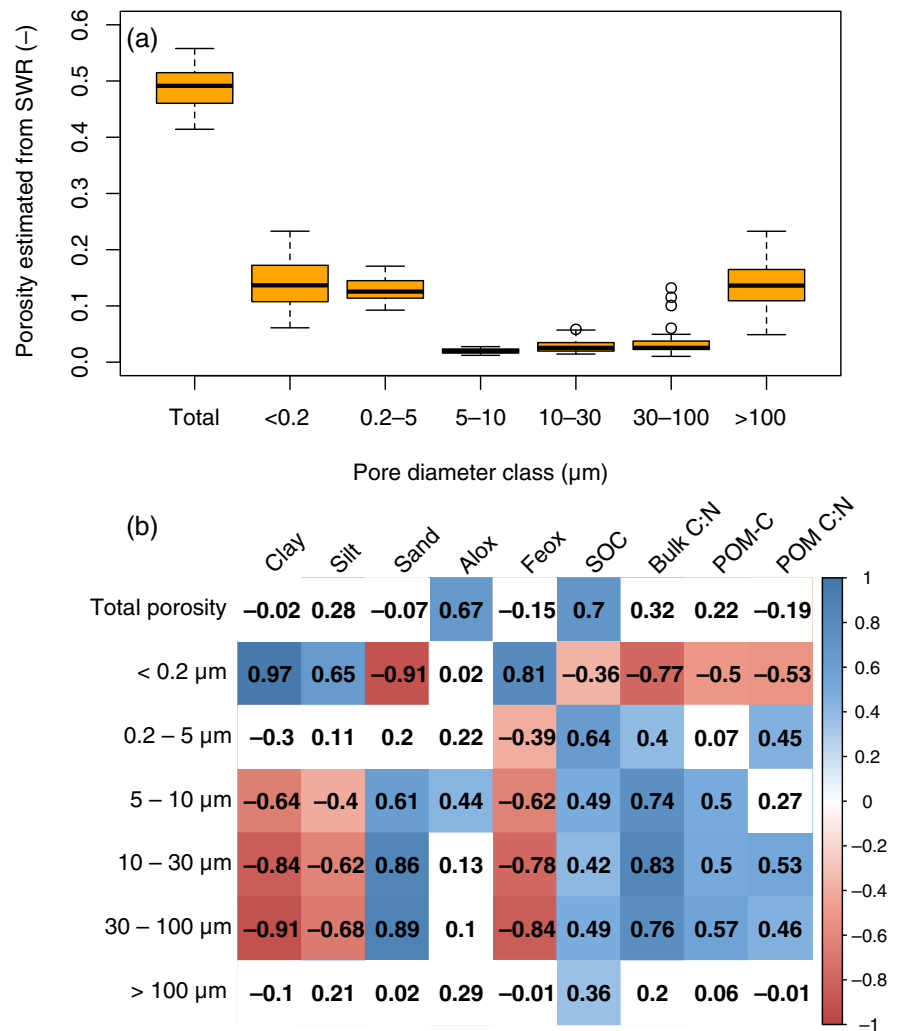
trend (Figure 6b). The relative contributions to the total explained variance for total porosity and porosities in the 0.2–5, 240–480 and 480–720 μm diameter classes were larger for SOC than for clay content, whereas the opposite was true for the other pore diameter classes (Figure 6c).

4 | DISCUSSION

4.1 | Macroporosity and bioporosity derived from X-ray tomography images

We found positive correlations between SOC and X-ray derived macroporosities in the 240–480 and 480–720 μm diameter classes. These results are consistent with results reported by Larsbo et al. (2016) and Xu et al. (2018), who observed positive correlations between SOC and porosity in the 200–600 μm diameter class and between SOM and porosity in the 200–500 μm diameter classes, respectively. Our SOM fractionation results showed that ca. 80% of

SOC was associated with the silt+clay sized (<63 μm) fraction (Figure 1b). However, mineral-associated SOC may still be important for the presence of pores in the 240–720 μm diameter classes by stabilising the macropore structure through clay-sized particle aggregation (Dexter et al., 2008; Fukumasu et al., 2021; Jensen et al., 2019). Another plausible explanation for the positive correlation between SOC and macropores in 240–720 μm diameter is that pores in this diameter class may be associated with meso-faunal activity and fine root growth (Bodner et al., 2014; Meurer, Barron, et al., 2020). Root-derived organic carbon also stimulates microbial and faunal activity in soil and contributes to the accumulation of stabilised or protected SOC (Kätterer et al., 2011; Kuzyakov & Blagodatskaya, 2015). However, bioporosities were not correlated with SOC content except for the 480–720 μm diameter class, which comprised a very small fraction of the total imaged porosity and hence would have limited effects on water dynamics and biogeochemical cycling. The inter-relationships between SOC, macropores, root abundance and microbial and
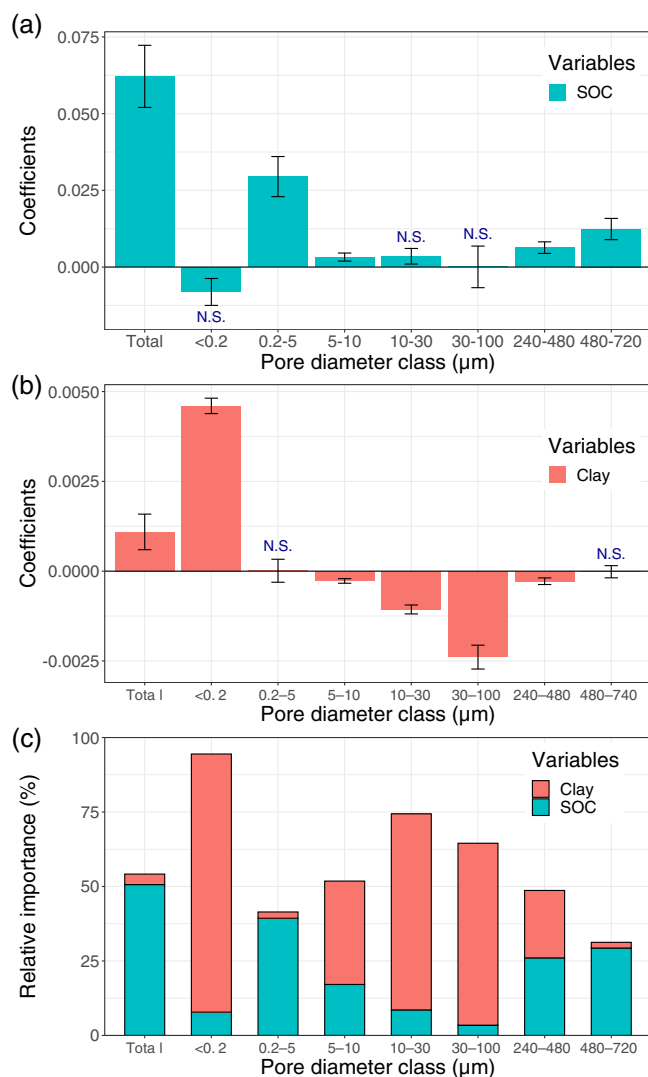
FIGURE 6 Coefficients of multiple linear regressions with (a) SOC (10 g kg^{-1} or %) and (b) clay (%) as explanatory variables and porosities derived from soil water retention measurements as response variable (error bars are standard error) and (c) relative contribution of SOC and clay contents to total explained variance for the multiple linear regression models. N.S. means that the coefficient was not significantly different from zero

faunal activity are still not well understood and should be further studied (Meurer, Barron, et al., 2020).

Neither porosities in the >720 μm diameter classes nor total X-ray visible macroporosity were correlated with total SOC and POM-C contents. This is in line with results of X-ray studies on other arable soils reported by Larsbo et al. (2016), Paradelo et al. (2016), Pituello et al. (2016), Jarvis et al. (2017) and Xu et al. (2018). Instead, macroporosity in the diameter classes of 1200–3120 μm was positively correlated with clay and silt contents. This may be due to the development of cracks (Paradelo et al., 2016) due to wetting and drying cycles, which result in swelling and shrinking in soils of

sufficient clay content (Colombi et al., 2021; Horn et al., 1994). Furthermore, the positive correlation between clay content, biopore length density and bioporosity in the 720–3120 μm diameter classes may be a consequence of the greater macro-faunal activity (e.g., earthworms) in loamy soils compared with sandy soils (Baker et al., 1998; Capowiez et al., 1998; Lindahl et al., 2009).

It should be noted that the total visible porosity was positively correlated with the porosities in all pore size classes (Figure S7). Similarly, total bioporosity was positively correlated with the bioporosities in all pore size classes except for the 480–720 μm diameter class (Figure S8). These results suggest that macropore and biopore formation did not cause redistribution of macropore and biopore sizes but instead contributed to increases in total macro- and bioporosities.

4.2 | Porosity and pore size distribution estimated by soil water retention

We found a significant positive correlation between SOC and total porosity, whereas total porosity was not correlated with soil texture (Figure 4b). These relations are well established at the field scale (e.g., Jarvis et al., 2017; Meurer, Chenu, et al., 2020; Paradelo et al., 2016) and at national and global scales (e.g., Kätterer et al., 2006; Nemes et al., 2005). Far fewer studies have reported relationships between SOC and PSDs and their results are much less clear (Lal, 2020; Minasny & McBratney, 2018a; Minasny & McBratney, 2018b). In our study, porosities in all classes except for pores <0.2 μm in diameter were positively correlated with SOC. In particular, the porosity in the 0.2–5 μm diameter class was strongly correlated with SOC. The porosity in this diameter class was not correlated with soil texture, while porosities in most of the other pore size classes were more strongly correlated with clay and sand contents than with SOC content. A plausible explanation for our results is that the formation of pores in the 0.2–5 μm diameter class may be governed by micro-aggregation of silt/clay size particles where physico-chemically protected SOC acts as a binding agent (Dexter et al., 2008; Jensen et al., 2019; Regelink et al., 2015). In a previous study using the same soils, we confirmed that the removal of SOC in the SC fraction led to the destruction of silt-sized (2–20 μm) aggregates and a release of clay-sized (<2 μm) particles, which indicated that SOC binds clay- and silt-sized particles together to form silt-sized micro-aggregates (Fukumasu et al., 2021). Also, microbial activity in the porosity in 0.2–5 μm diameter class may not be high because bacteria may not be able to colonise pore space of this size, which would

reduce the decomposition rate of SOC (Kravchenko et al., 2020; Kuzyakov & Blagodatskaya, 2015).

We found similarly strong positive correlations between SOC and porosities in the 1–5 μm and 0.2–30 μm diameter classes in an analysis of data presented in Kirchmann and Gerzabek (1999; Table S2) and Jensen et al. (2020; Table S3), respectively. Recently, Fu et al. (2021) also reported a strong positive correlation between SOC and porosity in the 0.2–7.5 μm diameter class in a regional scale study carried out in the Canterbury Plains in New Zealand. Interestingly, the causes of SOC variations in these studies were different from our field; the SOC gradient in the Bjertorp field was mostly explained by physico-chemical stabilisation mediated by reactive aluminium content and carbon input from crop production (Fukumasu et al., 2021), whereas the gradient in Kirchmann and Gerzabek (1999) was caused by various types of organic and inorganic fertilisers, the gradient in Jensen et al. (2020) was caused by land use changes between bare fallow, grassland and arable and the gradient in Fu et al. (2021) seemed to be caused by different land uses including irrigated arable fields and irrigated and non-irrigated pastures. On the other hand, Zhou et al. (2020) reported no correlation between SOC and 0.2–10 μm diameter porosity in a long-term fertilised Vertisol, whereas porosity <0.2 μm in diameter was positively correlated with SOC content. By quantifying a wide range of pore sizes (from nanopores (0.25–50 nm diameter) to meso- and macropores (> 25 μm diameter)) using different methods (X-ray tomography, mercury porosimetry and nitrogen gas adsorption) for soils from long-term experimental arable plots, Pituello et al. (2016) also reported that nanoporosity (10–50 nm diameter classes) was positively correlated with SOC, whereas meso- and macroporosities were not correlated with SOC except for the mesoporosity in the 30–75 μm diameter class, which was negatively correlated with SOC. The positive correlations between SOC and nanoporosity reported in these two studies indicate that SOC may be physically protected within such nanopores (Lützow et al., 2006; Mayer et al., 2004). The contrasting results between the studies cited above and the Bjertorp soils suggest that relations between SOC and PSD may be influenced by soil type (e.g., clay mineralogy) as reported in Libohova et al. (2018) and Lehmann et al. (2021).

The correlation analysis of the relationships between the porosities estimated from soil water retention showed that the increase of porosity smaller than 0.2 μm diameter was associated with the decreases of porosities in the 5–100 μm diameter classes (Figure S9). These pore size classes were strongly dependent on soil texture. This indicates that these pore size classes were associated with the abundance of textural pores (i.e., pores between primary particles), which is in line with the conceptual model proposed by Lucas et al. (2021).

4.3 | Responses of porosities to a unit increase of SOC and its implications for water dynamics

We found relatively large increases in porosities in the 0.2–5 and 480–720 μm diameter classes with a unit increase of SOC. In contrast, the porosities in the <0.2 and 5–100 μm diameter classes seem to be dominated by textural pores. The porosities in the 5–100 and 240–480 μm diameter classes decreased with higher clay contents while the porosities in the 5–10 and 240–480 μm increased with larger SOC content, which indicates that soils with larger clay contents need larger amounts of SOC to achieve a given soil porosity compared with soils with lower clay contents. These results fit with the concept that soils with higher clay content require higher SOC content to exhibit the same aggregate stability, soil structure quality score or clay dispersibility as compared with soil with lower clay contents (Feller & Beare, 1997; Johannes et al., 2017; Jones et al., 2021; Prout et al., 2021; Soinne et al., 2016).

The relationships between SOC contents and the porosities in the different pore size classes have implications for soil water dynamics. Based on the regression relationship in our study, a 10 g kg^{-1} increase in SOC content would result in an increase of about 3 mm 100 mm^{-1} soil depth for PAWC (i.e., the 0.2–10 μm diameter class). This is larger than the results of a meta-analysis (1.1–1.9 mm 100 mm^{-1} soil depth) by Minasny and McBratney (2018a). A relatively large increase of porosity associated with diameters between 480 and 720 μm with a unit increase of SOC content may increase unsaturated hydraulic conductivity and thus water flow through pores of this size, which may lead to a reduction in the risk of preferential flow (Larsbo et al., 2016).

4.4 | Reactive oxide phases, POM-C and C:N ratios

Porosities in some pore size classes were correlated with Feox, POM-C and Alox contents (Figure 5b). However, as shown in Figure 2, Feox and POM-C contents were strongly correlated with clay content, and SOC content was positively correlated with Alox content. Multiple linear regression analysis using clay and Alox or POM-C instead of SOC indicated that compared with SOC, Alox can better explain the variation of the porosity in the 5–10 μm diameter class and POM-C explains more of the

variation of the log-transformed porosity in 30–100 μm diameter class. Also, multiple linear regression analysis using SOC and Feox as explanatory variables showed that, in general, Feox did not improve the predictability of the porosities compared with the models with clay (data not shown). It should be noted that the contents of Feox (<8.8 g kg^{-1}), Alox (<2.1 g kg^{-1}) and POM-C (<3.4 g kg^{-1}) were much smaller than clay and SOC contents (Table S1). We therefore suggest that predictions of PSDs should be done using clay and SOC contents as predictors in our field. As reported in Fukumasu et al. (2021), Alox contents may instead be a key regulator for SOC stabilisation and clay aggregation in the Bjertorp field. Our results indicate that these reactive mineral phases have an indirect effect on soil pore structure via organo-mineral associations (Fukumasu et al., 2021).

Additionally, C:N ratios can be good indicators for the degree of microbial decomposition of SOM (Gregorich et al., 2006). We found positive correlations between C:N ratios of bulk SOM and/or POM and porosities in the 10–100 and 240–720 μm diameter classes, which indicates that such pores may be associated with less-microbially processed SOM. This is not in line with studies of Kravchenko et al. (2015) and Toosi et al. (2017), who reported that intra-aggregate POM and plant residues were rapidly decomposed when porosities in the >10 μm and >30 μm diameter classes were large. As discussed above, a plausible explanation for our results is that a larger abundance of pores in these diameter classes may be associated with higher growth of fine roots (Bodner et al., 2014), which may contribute to a supply of relatively fresh organic matter. However, since the C:N ratios and these porosities were also strongly correlated with soil texture, we cannot be certain that these pores were associated with the quality of SOM and POM.

5 | CONCLUSIONS

Within-field variations of SOC and clay contents enabled us to investigate their relations with PSDs under the same climate and similar land management. We found positive correlations between SOC content and porosities in the 0.2–720 μm diameter classes. In particular, the porosities in the 0.2–5 and 480–720 μm diameter classes were more strongly correlated with SOC than clay content. This highlights the potential importance of SOC for plant available water and unsaturated hydraulic conductivities. Multiple linear regression analysis also indicated that, to achieve a given soil porosity, samples with larger clay content would require larger SOC content compared with soils with lower clay content. Clay content may also determine the formation of large macropores and biopores through its effects on swelling and shrinking processes and soil macro-faunal activity (e.g., earthworms). Our results provide information on the potential effects of SOC sequestration in arable topsoil for soil PSDs, which may influence soil hydraulic properties, plant water supply and the physical conditions for root growth. Because our results, to a large extent, rely on correlations, the mechanisms behind interactions between SOC, biological activity and soil pore formation need to be further investigated in future studies.

CONFLICT OF INTEREST

The authors declare no conflict of interest.

DATA AVAILABILITY STATEMENT

The data that support the findings of this study are available from the corresponding author upon reasonable request.

AUTHOR CONTRIBUTIONS

Jumpei Fukumasu: Conceptualization (equal); formal analysis (lead); investigation (lead); methodology (equal); validation (lead); visualization (lead); writing – original draft (lead); writing – review and editing (equal). **Nick Jarvis:** Conceptualization (equal); funding acquisition (supporting); methodology (supporting); supervision (supporting); writing – review and editing (equal). **John Koestel:** Methodology (supporting); supervision (supporting); writing – review and editing (supporting). **Thomas Kätterer:** Conceptualization (supporting); funding acquisition (supporting); supervision (supporting); writing – review and editing (supporting). **Mats Larsbo:** Conceptualization (lead); funding acquisition (lead); investigation (supporting); methodology (lead); project administration (lead); resources (lead); supervision (lead); writing – review and editing (lead).

ORCID

Jumpei Fukumasu https://orcid.org/0000-0002-4875-1941

John Koestel https://orcid.org/0000-0002-3230-5699

REFERENCES

Abiven, S., Menasseri, S., & Chenu, C. (2009). The effects of organic inputs over time on soil aggregate stability: A literature analysis. *Soil Biology and Biochemistry*, 41, 1–12.

Asano, M., & Wagai, R. (2014). Evidence of aggregate hierarchy at micro- to submicron scales in an allophanic Andisol. *Geoderma*, 216, 62–74.

Baker, G. H., Carter, P. J., Curry, J. P., Cultreri, O., & Beck, A. (1998). Clay content of soil and its influence on the abundance of *Aporrectodea trapezoides* Dugès (Lumbricidae). *Applied Soil Ecology*, 9, 333–337.

Bodner, G., Leitner, D., & Kaul, H.-P. (2014). Coarse and fine root plants affect pore size distributions differently. *Plant and Soil*, 380, 133–151.

Bronick, C. J., & Lal, R. (2005). Soil structure and management: A review. *Geoderma*, 124, 3–22.

Capowiez, Y., Pierret, A., Daniel, O., Monestiez, P., & Kretzschmar, A. (1998). 3D skeleton reconstructions of natural earthworm burrow systems using CAT scan images of soil cores. *Biology and Fertility Soils*, 27, 51–59.

Chenu, C., Angers, D. A., Barré, P., Derrien, D., Arrouays, D., & Balesdent, J. (2019). Increasing organic stocks in agricultural soils: Knowledge gaps and potential innovations. *Soil and Tillage Research*, 188, 41–52.

Chenu, C., Le Bissonnais, Y., & Arrouays, D. (2000). Organic matter influence on clay wettability and soil aggregate stability. *Soil Science Society of America Journal*, 64, 1479–1486.

Colombi, T., Kirchgessner, N., Iseskog, D., Alexandersson, S., Larsbo, M., & Keller, T. (2021). A time-lapse imaging platform for quantification of soil crack development due to simulated root water uptake. *Soil and Tillage Research*, 205, 104769.

Dexter, A. R., Richard, G., Arrouays, D., Czyż, E. A., Jolivet, C., & Duval, O. (2008). Complexed organic matter controls soil physical properties. *Geoderma*, 144, 620–627.

Dungait, J. A. J., Hopkins, D. W., Gregory, A. S., & Whitmore, A. P. (2012). Soil organic matter turnover is governed by accessibility not recalcitrance. *Global Change Biology*, 18, 1781–1796.

Fell, V., Matter, A., Keller, T., & Boivin, P. (2018). Patterns and factors of soil structure recovery as revealed from a tillage and cover-crop experiment in a compacted orchard. *Frontiers in Environmental Science*, 6, 134.

Feller, C., & Beare, M. H. (1997). Physical control of soil organic matter dynamics in the tropics. *Geoderma*, 79, 69–116.

Franko, U., & Schulz, E. (2021). Carbon accumulation in a bare fallow Chernozem soil with high carbon input rates. *European Journal of Soil Science*, 72, 265–273.

Fu, Z., Hu, W., Beare, M., Thomas, S., Carrick, S., Dando, J., Langer, S., Müller, K., Baird, D., & Lilburne, L. (2021). Land use effects on soil hydraulic properties and the contribution of soil organic carbon. *Journal of Hydrology*, 602, 126741.

Fukumasu, J., Poeplau, C., Coucheney, E., Jarvis, N., Klöffel, T., Koestel, J., Kätterer, T., Nimblad Svensson, D., Wetterlind, J., & Larsbo, M. (2021). Oxalate-extractable aluminum alongside carbon inputs may be a major determinant for organic carbon content in agricultural topsoils in humid continental climate. *Geoderma*, 402, 115345.

Gregorich, E. G., Beare, M. H., McKim, U. F., & Skjemstad, J. O. (2006). Chemical and biological characteristics of physically uncomplexed organic matter. *Soil Science Society of America Journal*, 70, 975–985.

Grömping, U., & Lehrkamp, M. (2015). Package 'relaimpo': Relative importance of regressors in linear models. https://cran.r-project.org/web/packages/relaimpo.

Grønsten, H. A., & Børresen, T. (2009). Comparison of two methods for assessment of aggregate stability of agricultural soils in Southeast Norway. *Acta Agriculturae Scandinavica, Section B: Soil & Plant Science*, 59, 567–575.

Holmstrup, M., Lamandé, M., Torp, S. B., Greve, M. H., Labouriau, R., & Heckrath, G. (2011). Associations between soil texture, soil water characteristics and earthworm populations in grassland. *Acta Agriculturae Scandinavica Section B: Soil and Plant Science*, 61, 583–592.

Horn, R., Taubner, H., Wuttke, M., & Baumgartl, T. (1994). Soil physical properties related to soil structure. *Soil & Tillage Research*, 30, 187–216.

Hudson, B. D. (1994). Soil organic matter and available water capacity. *Journal of Soil and Water Conservation*, 49, 189–194.

Jarvis, N., Forkman, J., Koestel, J., Kätterer, T., Larsbo, M., & Taylor, A. (2017). Long-term effects of grass-clover leys on the structure of a silt loam soil in a cold climate. *Agriculture, Ecosystems and Environment*, 247, 319–328.

Jastrow, J. D., Amonette, J. E., & Bailey, V. L. (2007). Mechanisms controlling soil carbon turnover and their potential application for enhancing carbon sequestration. *Climatic Change*, 80, 5–23.

Jensen, J. L., Schjønning, P., Watts, C. W., Christensen, B. T., & Munkholm, L. J. (2020). Short-term changes in soil pore size distribution: Impact of land use. *Soil and Tillage Research*, 199, 104597.

Jensen, J. L., Schjønning, P., Watts, C. W., Christensen, B. T., Peltre, C., & Munkholm, L. J. (2019). Relating soil C and organic matter fractions to soil structural stability. *Geoderma*, 337, 834–843.

Johannes, A., Matter, A., Schulin, R., Weisskopf, P., Baveye, P. C., & Boivin, P. (2017). Optimal organic carbon values for soil structure quality of arable soils. Does clay content matter? *Geoderma*, 302, 14–21.

Jones, E. J., Filippi, P., Wittig, R., Fajardo, M., Pino, V., & McBratney, A. B. (2021). Mapping soil slaking index and assessing the impact of management in a mixed agricultural landscape. *Soil*, 7, 33–46.

Kätterer, T., Andrén, O., & Jansson, P. E. (2006). Pedotransfer functions for estimating plant available water and bulk density in Swedish agricultural soils. *Acta Agriculturae Scandinavica Section B: Soil and Plant Science*, 56, 263–276.

Kätterer, T., Bolinder, M. A., Andrén, O., Kirchmann, H., & Menichetti, L. (2011). Roots contribute more to refractory soil organic matter than above-ground crop residues, as revealed by a long-term field experiment. *Agriculture, Ecosystems and Environment*, 141, 184–192.

King, A. E., Congreves, K. A., Deen, B., Dunfield, K. E., Voroney, R. P., & Wagner-Riddle, C. (2019). Quantifying the relationships between soil fraction mass, fraction carbon, and total soil carbon to assess mechanisms of physical protection. *Soil Biology and Biochemistry*, 135, 95–107.

Kirchmann, H., & Gerzabek, M. H. (1999). Relationship between soil organic matter and micropores in a long-term experiment

at Ultuna, Sweden. *Journal of Plant Nutrition and Soil Science*, *162*, 493–498.

Klok, C., Faber, J., Heijmans, G., Bodt, J., & van der Hout, A. (2007). Influence of clay content and acidity of soil on development of the earthworm *Lumbricus rubellus* and its population level consequences. *Biology and Fertility Soils*, *43*, 549–556.

Koestel, J. (2018). SoilJ: An ImageJ plugin for the semiautomatic processing of three-dimensional X-ray images of soils. *Vadose Zone Journal*, *17*, 170062.

Kravchenko, A. N., & Guber, A. K. (2017). Soil pores and their contributions to soil carbon processes. *Geoderma*, *287*, 31–39.

Kravchenko, A. N., Guber, A. K., Razavi, B. S., Koestel, J., Quigley, M. Y., Robertson, G. P., & Kuzyakov, Y. (2020). Reply to: "Variables in the effect of land use on soil extrapore enzymatic activity and carbon stabilization" by Glenn (2020). *Nature Communications*, *11*, 6427.

Kravchenko, A. N., Negassa, W. C., Guber, A. K., & Rivers, M. L. (2015). Protection of soil carbon within macro-aggregates depends on intra-aggregate pore characteristics. *Scientific Reports*, *5*, 16261.

Kuzyakov, Y., & Blagodatskaya, E. (2015). Microbial hotspots and hot moments in soil: Concept & review. *Soil Biology and Biochemistry*, *83*, 184–199.

Lal, R. (2020). Soil organic matter and water retention. *Agronomy Journal*, *112*, 3265–3277.

Larsbo, M., Koestel, J., & Jarvis, N. (2014). Relations between macropore network characteristics and the degree of preferential solute transport. *Hydrology and Earth System Science*, *18*, 5255–5269.

Larsbo, M., Koestel, J., Kätterer, T., & Jarvis, N. (2016). Preferential transport in macropores is reduced by soil organic carbon. *Vadose Zone Journal*, *15*, 1–17.

Lavallee, J. M., Soong, J. L., & Cotrufo, M. F. (2020). Conceptualizing soil organic matter into particulate and mineral-associated forms to address global change in the 21st century. *Global Change Biology*, *26*, 261–273.

Le Couteulx, A., Wolf, C., Hallaire, V., & Pérès, G. (2015). Burrowing and casting activities of three endogeic earthworm species affected by organic matter location. *Pedobiologia*, *58*, 97–103.

Lehmann, P., Leshchinsky, B., Gupta, S., Mirus, B. B., Bickel, S., Lu, N., & Or, D. (2021). Clays are not created equal: How clay mineral type affects soil parameterization. *Geophysical Research Letters*, *48*, e2021GL095311.

Libohova, Z., Seybold, C., Wysocki, D., Wills, S., Schoeneberger, P., Williams, C., Lindbo, D., Stott, D., & Owens, P. R. (2018). Reevaluating the effects of soil organic matter and other properties on available water-holding capacity using the National Cooperative Soil Survey Characterization Database. *Journal of Soil and Water Conservation*, *73*, 411–421.

Lindahl, A. M. L., Dubus, I. G., & Jarvis, N. J. (2009). Site classification to predict the abundance of the deep-burrowing earthworm *Lumbricus terrestris* L. *Vadose Zone Journal*, *8*, 911–915.

Lindahl, A. M. L., Söderström, M., & Jarvis, N. (2008). Influence of input uncertainty on prediction of within-field pesticide leaching risks. *Journal of Contaminant Hydrology*, *98*, 106–114.

Lucas, M., Schlüter, S., Vogel, H.-J., & Vetterlein, D. (2019). Soil structure formation along an agricultural chronosequence. *Geoderma*, *350*, 61–72.

Lucas, M., Vetterlein, D., Vogel, H.-J., & Schlüter, S. (2021). Revealing pore connectivity across scales and resolutions with X-ray CT. *European Journal of Soil Science*, *72*, 546–560.

Lützow, M. V., Kögel-Knabner, I., Ekschmitt, K., Matzner, E., Guggenberger, G., Marschner, B., & Flessa, H. (2006). Stabilization of organic matter in temperate soils: Mechanisms and their relevance under different soil conditions: A review. *European Journal of Soil Science*, *57*, 426–445.

Mayer, L. M., Schick, L. L., Hardy, K. R., Wagai, R., & McCarthy, J. (2004). Organic matter in small mesopores in sediments and soils. *Geochimica et Cosmochimica Acta*, *68*, 3863–3872.

Meurer, K., Barron, J., Chenu, C., Coucheney, E., Fielding, M., Hallett, P., Herrmann, A. M., Keller, T., Koestel, J., Larsbo, M., Lewan, E., Or, D., Parsons, D., Parvin, N., Taylor, A., Vereecken, H., & Jarvis, N. (2020). A framework for modelling soil structure dynamics induced by biological activity. *Global Change Biology*, *26*, 5382–5403.

Meurer, K., Chenu, C., Coucheney, E., Herrmann, A., Keller, T., Kätterer, T., Nimblad Svensson, D., & Jarvis, N. (2020). Modelling dynamic interactions between soil structure and the storage and turnover of soil organic matter. *Biogeosciences*, *17*, 5025–5042.

Minasny, B., & McBratney, A. B. (2018a). Limited effect of organic matter on soil available water capacity. *European Journal of Soil Science*, *69*, 39–47.

Minasny, B., & McBratney, A. B. (2018b). Rejoinder to the comment on: B. Minasny & A.B. McBratney. 2018. Limited effect of organic matter on soil available water capacity. *European Journal of Soil Science*, *69*, 155–157.

Naveed, M., Moldrup, P., Vogel, H.-J., Lamandé, M., Wildenschild, D., Tuller, M., & de Jonge, L. W. (2014). Impact of long-term fertilization practice on soil structure evolution. *Geoderma*, *217-218*, 181–189.

Nemes, A., Rawls, W. J., & Pachepsky, Y. A. (2005). Influence of organic Matter on the estimation of saturated hydraulic conductivity. *Soil Science Society of America Journal*, *69*, 1330–1337.

Olness, A., & Archer, D. (2005). Effect of organic carbon on available water in soil. *Soil Science*, *170*, 90–101.

Paradelo, M., Katuwal, S., Moldrup, P., Norgaard, T., Herath, L., & de Jonge, L. W. (2016). X-ray CT-derived soil characteristics explain varying air, water, and solute transport properties across a loamy field. *Vadose Zone Journal*, *15*, 1–13.

Pituello, C., Dal Ferro, N., Simonetti, G., Berti, A., & Morari, F. (2016). Nano to macro pore structure changes induced by long-term residue management in three different soils. *Agriculture, Ecosystems & Environment*, *217*, 49–58.

Poeplau, C., Don, A., Dondini, M., Leifeld, J., Nemo, R., Schumacher, J., Senapati, N., & Wiesmeier, M. (2013). Reproducibility of a soil organic carbon fractionation method to derive RothC carbon pools. *European Journal of Soil Science*, *64*, 735–746.

Poeplau, C., Don, A., Six, J., Kaiser, M., Benbi, D., Chenu, C., Cotrufo, M. F., Derrien, D., Gioacchini, P., Grand, S., Gregorich, E., Griepentrog, M., Gunina, A., Haddix, M., Kuzyakov, Y., Kühnel, A., Macdonald, L. M., Soong, J., Trigalet, S., ... Nieder, R. (2018). Isolating organic carbon fractions with varying turnover rates in temperate agricultural

soils: A comprehensive method comparison. *Soil Biology and Biochemistry*, *125*, 10–26.

Poeplau, C., & Kätterer, T. (2017). Is soil texture a major controlling factor of root: shoot ratio in cereals? *European Journal of Soil Science*, *68*, 964–970.

Prout, J. M., Shepherd, K. D., McGrath, S. P., Kirk, G. J. D., & Haefele, S. M. (2021). What is a good level of soil organic matter? An index based on organic carbon to clay ratio. *European Journal of Soil Science*, *72*, 2493–2503.

R Core Team. (2019). *R: A language and environment for statistical computing*. R foundation for statistical computing https://www.R-project.org/

Rabot, E., Wiesmeier, M., Schlüter, S., & Vogel, H. J. (2018). Soil structure as an indicator of soil functions: A review. *Geoderma*, *314*, 122–137.

Rawls, W. J., Pachepsky, Y. A., Ritchie, J. C., Sobecki, T. M., & Bloodworth, H. (2003). Effect of soil organic carbon on soil water retention. *Geoderma*, *116*, 61–76.

Regelink, I. C., Stoof, C. R., Rousseva, S., Weng, L., Lair, G. J., Kram, P., Nikolaidis, N. P., Kercheva, M., Banwart, S., & Comans, R. N. J. (2015). Linkages between aggregate formation, porosity and soil chemical properties. *Geoderma*, *247*, 24–37.

Rocci, K. S., Lavallee, J. M., Stewart, C. E., & Cotrufo, M. F. (2021). Soil organic carbon response to global environmental change depends on its distribution between mineral-associated and particulate organic matter: A meta-analysis. *Science of The Total Environment*, *793*, 148569.

Ruamps, L. S., Nunan, N., & Chenu, C. (2011). Microbial biogeography at the soil pore scale. *Soil Biology and Biochemistry*, *43*, 280–286.

Ruehlmann, J., & Körschens, M. (2009). Calculating the effect of soil organic matter concentration on soil bulk density. *Soil Science Society of America Journal*, *73*, 876–885.

Schindelin, J., Arganda-Carreras, I., Frise, E., Kaynig, V., Longair, M., Pietzsch, T., Preibisch, S., Rueden, C., Saalfeld, S., Schmid, B., Tinevez, J.-Y., White, D. J., Hartenstein, V., Eliceiri, K., Tomancak, P., & Cardona, A. (2012). Fiji: An open-source platform for biological-image analysis. *Nature Methods*, *9*, 676–682.

Shoji, S., Nanzyo, M., Dahlgren, R. A., & Quantin, P. (1996). Evaluation and proposed revisions of criteria for andosols in the world reference base for soil resources. *Soil Science*, *161*, 604–615.

Six, J., Bossuyt, H., Degryze, S., & Denef, K. (2004). A history of research on the link between (micro)aggregates, soil biota, and soil organic matter dynamics. *Soil and Tillage Research*, *79*, 7–31.

Soinne, H., Hyväluoma, J., Ketoja, E., & Turtola, E. (2016). Relative importance of organic carbon, land use and moisture conditions for the aggregate stability of post-glacial clay soils. *Soil and Tillage Research*, *158*, 1–9.

Strong, D. T., Wever, H. D., Merckx, R., & Recous, S. (2004). Spatial location of carbon decomposition in the soil pore system. *European Journal of Soil Science*, *55*, 739–750.

Toosi, E. R., Kravchenko, A. N., Guber, A. K., & Rivers, M. L. (2017). Pore characteristics regulate priming and fate of carbon from plant residue. *Soil Biology and Biochemistry*, *113*, 219–230.

Totsche, K. U., Amelung, W., Gerzabek, M. H., Guggenberger, G., Klumpp, E., Knief, C., Lehndorff, E., Mikutta, R., Peth, S., Prechtel, A., Ray, N., & Kögel-Knabner, I. (2018). Microaggregates in soils. *Journal of Plant Nutrition and Soil Science*, *181*, 104–136.

Xu, L. Y., Wang, M. Y., Shi, X. Z., Yu, Q. B., Shi, Y. J., Xu, S. X., & Sun, W. X. (2018). Effect of long-term organic fertilization on the soil pore characteristics of greenhouse vegetable fields converted from rice-wheat rotation fields. *Science of the Total Environment*, *631-632*, 1243–1250.

Zacharias, S., & Wessolek, G. (2007). Excluding organic matter content from pedotransfer predictors of soil water retention. *Soil Science Society of America Journal*, *71*, 43–50.

Zhou, H., Chen, C., Wang, D., Arthur, E., Zhang, Z., Guo, Z., Peng, X., & Mooney, S. J. (2020). Effect of long-term organic amendments on the full-class soil water retention characteristics of a vertisol. *Soil and Tillage Research*, *202*, 104663.

Zimmermann, M., Leifeld, J., Schmidt, M. W. I., Smith, P., & Fuhrer, J. (2007). Measured soil organic matter fractions can be related to pools in the RothC model. *European Journal of Soil Science*, *58*, 658–667.

SUPPORTING INFORMATION

Additional supporting information may be found in the online version of the article at the publisher's website.